September 10-14, 2012 , Vienna, Austria

ECCOMAS 2012

European Congress on Computational Methods
in Applied Sciences and Engineering

Anisotropic Goal-oriented estimate for a third-order accurate Euler model

Alexandre Carabias[†], **Anca Belme**[†], **Frédéric Alauzet**[‡], **Adrien Loseille**[‡], **Alain Dervieux**[†]

([†]) INRIA - Tropics project Sophia-Antipolis, France
([‡])INRIA - Gamma Project Rocquencourt, France
Alexandre.Carabias@inria.fr

Motivation of the study

- Propagation of waves in large spaces.
- Mesh adaptation would follow the wave propagation.
- Adjoint-based adaptation criterion will concentrate on zone of interest for a chosen functional output.
- An accurate approximation scheme needs be chosen.

Scope of the talk

1. CENO2 Scheme
2. Error analysis
3. Optimal metric
4. Resolution of optimum
5. Numerical experiments
6. Concluding remarks

1. CENO2 Scheme (1)

Vertex, dual cell, 2-exact Central-ENO* quadratic reconstruction

Given $\bar{u}_i$ on on each cell i of centroid G_i, find the $c_{i,\alpha}$, $|\alpha| \leq$ **2** s.t.

$$R_2^0 \bar{u}_i(x) = \bar{u}_i + \sum_{|\alpha|\leq 2} c_{i,\alpha}\left[(X - G_i)^\alpha - \int_{Cell_i} (X - G_i)^\alpha \mathrm{d}\mathbf{x}\right]$$

$$\overline{R_2^0 \bar{u}} = \int_{Cell_i} R_2^0 \bar{u}_{i,i} \mathrm{d}\mathbf{x} = \overline{u_i} \qquad \sum_{j \in N(i)} (\overline{R_2^0 \bar{u}_{i,j}} - \overline{u_j})^2 = Min\ .$$

* after C. Groth.

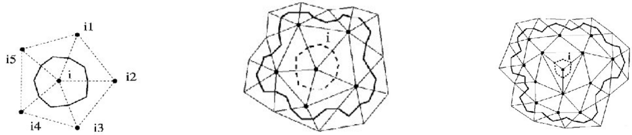

1. CENO2 Scheme (1)

Variational statement of discrete CENO2 scheme

$$B(u,v) = \int_\Omega v \nabla \cdot \mathcal{F}(u) \, \mathrm{d}\Omega \quad ; \quad F(u,v) = \int_\Gamma v \mathcal{F}_\Gamma(u) \, \mathrm{d}\Gamma,$$

Find $u \in \mathcal{V}$ such that $B(u,v) = F(u,v) \; \forall \; v \in \mathcal{V}$.

$$\mathcal{V}_0 = \{v_0, V_0|_{Cell_i} = const \; \forall \; i\}$$

CENO discrete statement:

Find $u_0 \in \mathcal{V}_0$ such that $B(R_2^0 u_0, v_0) = F(R_2^0 u_0, v_0) \; \forall \; v_0 \in \mathcal{V}_0$

1. CENO2 Scheme (2)

2-exact flux integration

The integral on a cell interface $C_{ij} = C_i \cap C_j$ is split into the integrals on the two segments of C_{ij}.

On each segment $C_{ij}^{(1)}$ and $C_{ij}^{(2)}$ a numerical integration with two Gauss points (two Riemann solvers) is applied.

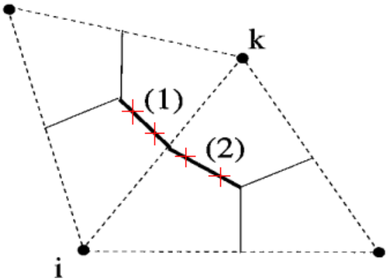

1. CENO2 Scheme (4)

Computational accuracy

The scheme is third order accurate when combined with a third-order time advancing (RK3).

The Quadratic-CENO scheme involves a fourth-order dissipation with Δx^3 weight term,*i.e.* of same order as for a MUSCL second-order scheme.

The number of Riemann solvers to compute is 4 times larger than for a MUSCL second-order scheme.

CENO2 is too dissipative

A test case: C.Tam's test for linear acoustics

[Ouvrard-Kozubskaya-Abalakin-Koobus-Dervieux, INRIA Rep. 2009]

- 12 Δx per bandwidth, three types of mesh.
- **black**: MUSCLV6 scheme, **Blue**: the present CENO2 scheme.

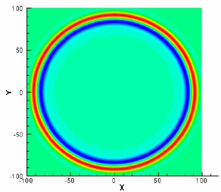

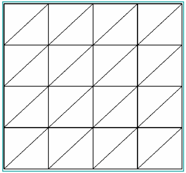

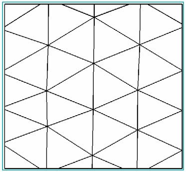

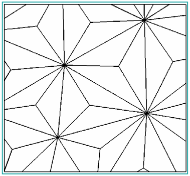

Mesh1	Mesh1	Mesh2	Mesh2	Mesh3	Mesh3
L^1	L^2	L^1	L^2	L^1	L^2
1.3045D-3	2.8561D-3	1.2786D-3	2.6318D-3	3.1097D-3	5.9216D-3
1.5189D-4	3.4010D-4	3.7384D-4	2.6318D-3	6.7626D-4	1.4598D-3

Computational accuracy

A variant of the Quadratic-CENO scheme uses:

- central differencing for the Gauss points integration instead of a Riemann solver and

- an added 6-th order dissipation in order to ensure some robustness.

From left to right: basic CENO2, centered CENO2, new CENO2 schemes.

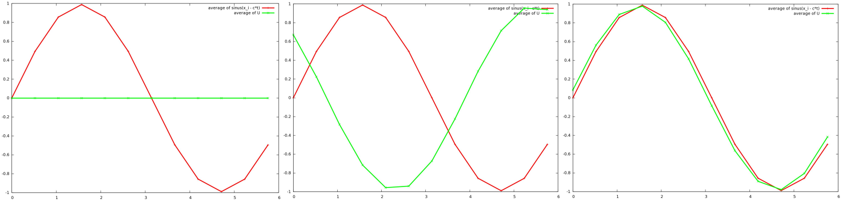

Exact solution, Numerical solution.

2. *A priori* error analysis (1)

Cf. *A posteriori* analysis for a large set of p-order reconstruction-based Godunov methods: Barth-Larson 2002.

Find $u_0 \in \mathcal{V}_0$ such that $B(R_p^0 u_0, v_0) = F(R_p^0 u_0, v_0) \ \forall \ v_0 \in \mathcal{V}_0$

$j(u) = (g, u)$: scalar output. $\quad \delta j = (g, R_p^0 \pi_0 u - R_p^0 u_0)$.

The adjoint state $u_0^* \in \mathcal{V}_0$ is the solution of:

$$\frac{\partial(B - F)}{\partial u}(R_p^0 u_0)(R_p^0 v_0, u_0^*) = (g, R_p^0 v_0), \ \forall \ v_0 \in \mathcal{V}_0.$$

We also need to define the projection π_0:

$$\pi_0 : (V) \to (V_0), \ \ v \mapsto \pi_0 v \forall \ C_i, \text{dual cell}, \pi_0 v|_{C_i} = \int_{C_i} v dx.$$

2. *A priori* error analysis (2)

Simpler case:

B is bilinear, F is linear, for example:
$B(u,v) = \int_\Omega v div \mathbf{V} u d\Omega + \int_\Gamma uv\mathbf{V}\cdot\mathbf{n}d\Gamma$ and $F(v) = \int_\Gamma u_B v\mathbf{V}\cdot\mathbf{n}d\Gamma$.

$$\begin{array}{rcll} B(v,u_0^*) & = & (g,v) & \text{(discr.adj. eq.)} \\ B(R_p^0 u_0, v) & = & F(v) & \text{(discr.state eq.)} \\ B(u,v) & = & F(v) & \text{(cont.state eq.)} \end{array}$$

$\Rightarrow$

$$\begin{array}{rcll} (g, R_p^0\pi_0 u - R_p^0 u_0) & = & B(R_p^0\pi_0 u - R_p^0 u_0, u_0^*) & \text{(discr.adj. eq.)} \\ & \approx & B(R_p^0\pi_0 u, u_0^*) - B(R_p^0 u_0, u_0^*) & \\ & \approx & B(R_p^0\pi_0 u, u_0^*) - F(u_0^*) & \text{(discr.state eq.)} \\ & \approx & B(R_p^0\pi_0 u, u_0^*) - B(u, u_0^*) & \text{(cont.state eq.)} \\ & \approx & B(R_p^0\pi_0 u - u, u_0^*) & \end{array}$$

The error is directly expressed in terms of the reconstruction error for exact solution, essentially the rest of a Taylor formula.

2. *A priori* error analysis (3)

Unsteady Euler: $W = (\rho, \rho u, \rho v, \rho E)$

For the case of Euler eqs, we get after some calculations:

$$|B(R_p^0 \pi_0 W - W, W_0^*)| \approx\leq 2 \int_\Omega \sum_q K_q(W, W^*) |G(u_q^{(p+1)}, (\delta \mathbf{x})^{p+1})| \, \mathrm{d}\Omega$$

with $(u_q)_{q=1,8} = (W, W_t)$.

3. Optimal metric (1)

The parametrization of the mesh is a Riemannian metric defined in each point **x** of the computational domain by a symmetric matrix,

$$\mathcal{M}(\mathbf{x}) = \mathcal{R}(\mathbf{x})\bar{\Lambda}(\mathbf{x})\mathcal{R}^t(\mathbf{x}) = d_{\mathcal{M}}\mathcal{R}(\mathbf{x})\Lambda(\mathbf{x})\mathcal{R}^t(\mathbf{x}).$$

• $\mathcal{R} = (\mathbf{e}_\xi, \mathbf{e}_\eta)$ is the rotation matrix built with the normalised eigenvectors of $\mathcal{M}$, parametrises the two orthogonal stretching directions of the metric.

• $\bar{\Lambda}$ is a 2×2 diagonal matrix with eigenvalues $\bar{\lambda}_1 = (m_\xi)^{-2}$ and $\bar{\lambda}_2 = (m_\eta)^{-2}$ where m_ξ and m_η represent the two directional local mesh sizes in the characteristic/stretching directions of $\mathcal{M}$.

• Λ is the diagonal matrix with eigenvalues $\lambda_1 = m_\eta/m_\xi$ and $\lambda_2 = m_\xi/m_\eta$ and $det\ \Lambda = 1$.

• $d_{\mathcal{M}} = m_\xi^{-1} m_\eta^{-1}$ is the node density.

3. Optimal metric (2)

Given a metric or -somewhat equivalently- a mesh described by it, we modelise the quadratic interpolation error like in the communication of Mbinky *et al.*:

$$|u_q(\mathbf{x}) - \pi_p u_q(\mathbf{x})| = \left(|\frac{\partial^{p+1} u_q}{\partial \tau_q^{p+1}}|^{\frac{2}{p}} (\delta \tau_q^{\mathcal{M}})^2 + |\frac{\partial^{p+1} u_q}{\partial n_q^{p+1}}|^{\frac{2}{p}} (\delta n_q^{\mathcal{M}})^2 \right)^{\frac{p}{2}}$$

$$= \left(trace(\mathcal{M}^{-1/2} S_q \mathcal{M}^{-1/2}) \right)^{\frac{p}{2}} .$$

For the MUSCL scheme, p=1:

$$|u_q(\mathbf{x}) - \pi_1 u_q(\mathbf{x})| = |\frac{\partial^{p+1} u_q}{\partial \tau_q^{p+1}}| (\delta \tau_q^{\mathcal{M}})^2 + |\frac{\partial^{p+1} u_q}{\partial n_q^{p+1}}| (\delta n_q^{\mathcal{M}})^2$$

For the CENO2 scheme, p=2:

$$|u_q(\mathbf{x}) - \pi_2 u_q(\mathbf{x})| = \left(|\frac{\partial^3 u_q}{\partial \tau_q^3}|^{\frac{2}{3}} (\delta \tau_q^{\mathcal{M}})^2 + |\frac{\partial^3 u_q}{\partial n_q^3}|^{\frac{2}{3}} (\delta n_q^{\mathcal{M}})^2 \right)^{\frac{3}{2}} .$$

3. Optimal metric (3)

After the *a priori* analysis, we have to minimise the following error:

$$\mathcal{E} = \int \sum_q K_q(W, W^*) \left(trace(\mathcal{M}^{-1/2} S_q \mathcal{M}^{-1/2}) \right)^{\frac{p}{2}} \; dxdy$$

$$= \int \left(trace(\mathcal{M}^{-1/2} S \mathcal{M}^{-1/2}) \right)^{\frac{p}{2}} \; dxdy$$

$$= \int d_{\mathcal{M}}^{-\frac{p}{2}} \left(trace(\mathcal{R}_{\mathcal{M}} \Lambda_{\mathcal{M}} \mathcal{R}_{\mathcal{M}}^T)^{-\frac{1}{2}} |S| (\mathcal{R}_{\mathcal{M}} \Lambda_{\mathcal{M}} \mathcal{R}_{\mathcal{M}}^T)^{-\frac{1}{2}}) \right)^{\frac{p}{2}} \; dxdy$$

$$\text{with constraint} \int d_{\mathcal{M}} \; dxdy = N.$$

Optimal solution:

$\forall$ $\mathbf{x}$ $: S = \mathcal{R}_S \bar{\Lambda}_S \mathcal{R}_S^T \;\Rightarrow\; \mathcal{R}_{\mathcal{M}_{opt}} = \mathcal{R}_S \;,\; \Lambda_{\mathcal{M}_{opt}} = \bar{\Lambda}_S^{-1} / det(S)$

$det(S)^{\frac{p}{2}} (d_{\mathcal{M}_{opt}})^{-\frac{p+1}{2}} = const.$

$\Rightarrow \; d_{\mathcal{M}_{opt}} \; = \; N \left(\int det(S)^{\frac{p+1}{p+3}} \; dxdy \right)^{-1} det(S)^{\frac{2}{p+1}}$

The *continuous* model giving the adapted mesh involves a **state system**, an **adjoint system** and the **optimality relation** giving $\mathcal{M}_{opt}$.

We discretise it.

The time discretisation of the metric is made of coarser time intervals.

We solve it.

... by the Global Unsteady Fixed Point algorithm of Belme *et al.*.

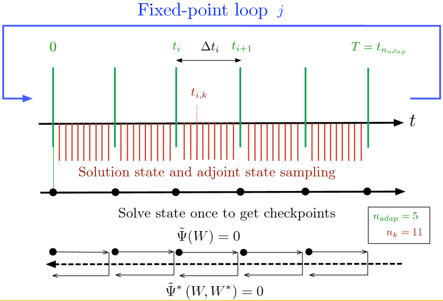

5. Numerical experiments

We present a first series of experiments where the propagation of an acoustical perturbation is followed by the mesh adaptator in order to minimise the mesh effort.

1. Noise wall problem
2. Difraction problem

5. Numerical experiments: Noise wall problem (1)

Propagation of an acoustic wave from a source while observing the impact on the detector.

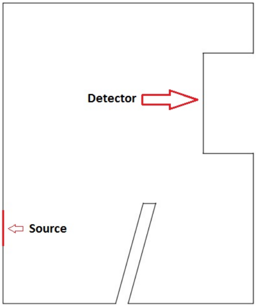

Acoustic source :

$$r = -Ae^{-Bln(2)\left[x^2+y^2\right]}cos(2\pi f).$$

Functional:

$$j(W) = \int_0^T \int_M \frac{1}{2}(p - p_{air})^2 \mathrm{d}M\mathrm{d}t.$$

5. Numerical experiments: Noise wall problem (2)

Density field evolving in time on uniform mesh (line 1), adapted one (middle line), with corresponding adapted meshes (last line):

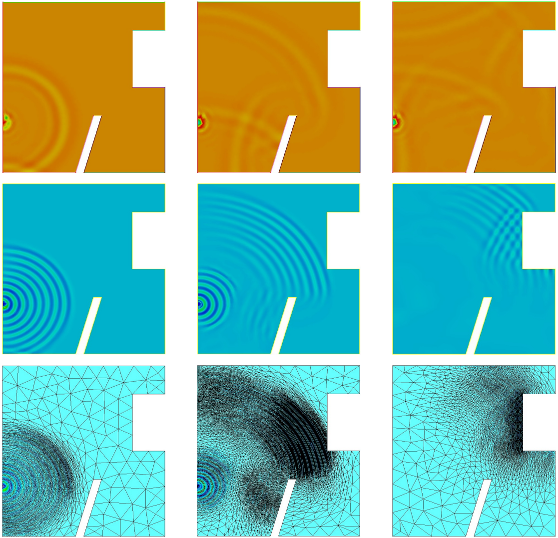

5. Numerical experiments: Noise wall problem (3)

Scalar output comparaison : MUSCL (-) vs CENO (—) schemes.

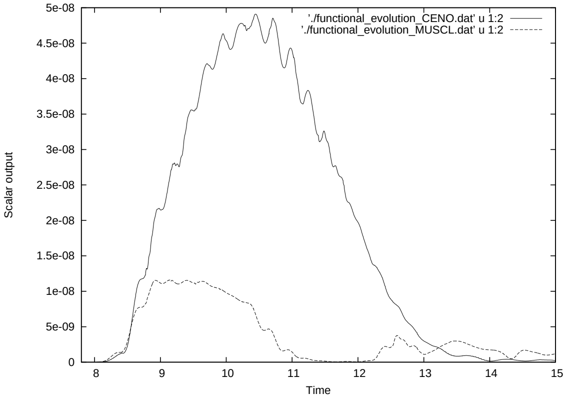

The difraction of an acoustic wave travelling from a source location to a detector situated in a small region under the "step".

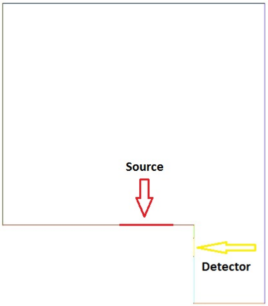

Acoustic source :

$$r = -Ae^{-Bln(2)\left[x^2+y^2\right]} cos(2\pi f).$$

Functional:

$$j(W) = \int_0^T \int_M \frac{1}{2}(p - p_{air})^2 \mathrm{d}M\mathrm{d}t.$$

5. Numerical experiments: Difraction problem (2)

Density field evolving in time on uniform mesh (line 1), adapted one (middle line), with corresponding adapted meshes (last line):

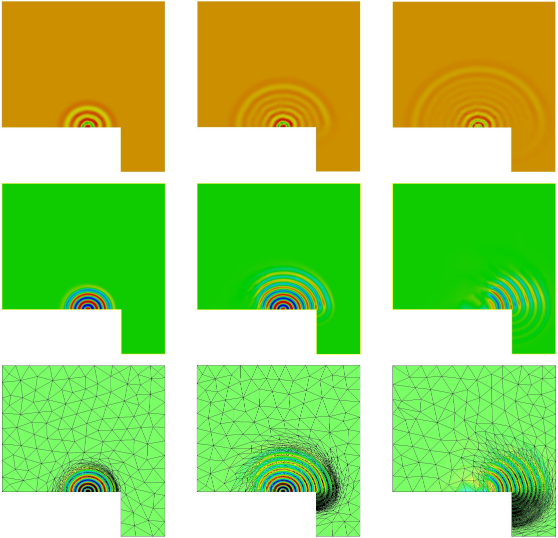

5. Numerical experiments: Difraction problem (3)

- Our goal-oriented method ensures the accuracy of the functional output $j(W) = \int_0^T \int_M \frac{1}{2}(p - p_{air})^2 \mathrm{d}M\mathrm{d}t$.

- It is thus interesting to analyse the integrand $k(t) = \int_M \frac{1}{2}(p - p_{air})^2 \mathrm{d}M$ of $j(W)$ on the micro M for different sizes of uniform vs. adapted meshes.

Functional time integrand calculation on different sizes of non-adapted meshes (28K, 40K, 68K) vs. adapted meshes (mean sizes: 2620, 4892, 6130).

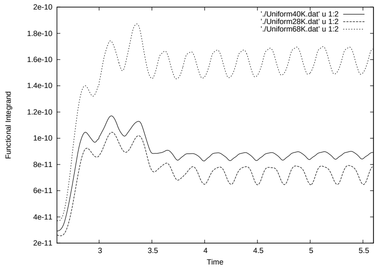

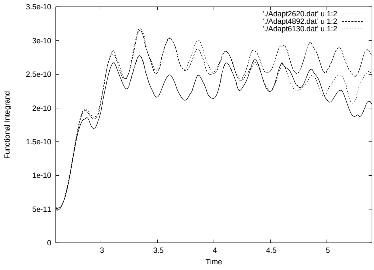

The convergence order is found to be 0.6 for uniform meshes and 1.98 for the adapted one.

6. Concluding remarks (1)

A third-order (spatially) accurate goal-oriented mesh adaptation method has been built on the basis of:

• The extension of Hessian analysis to higher order interpolation of Mbinky *et al.*.
• A novel *a priori* analysis.
• The Unsteady Global Fixed-Point mesh adaptation algorithm of Belme *et al.* .

Numerical experiments are yet only 2D and at the very beginning.

7. Concluding remarks (2)

Next studies will address:

- Steady test cases.
- Flows with singularities.
- 3D extension.


MERCI!
THANK YOU!
FRAPAR.